

A FAST ANALYSIS OF SCATTERING FROM MICROSTRIP ANTENNAS OVER A WIDE BAND

J. X. Wan, C. H. Liang, and J. Lei

The Department of Electronics Engineering
XiDian University
Xi'an 710071, P. R. China

Abstract—An efficient algorithm combining the fast multipole method (FMM) and the characteristic basis function method (CBFM) for analysis of scattering from microstrip antennas over a wide band is introduced in this paper. In the hybrid algorithm, the characteristic basis function method is used to construct the currents on microstrip antennas by using characteristic basis functions (CBFs) which are constructed from the solution vectors at several samples using the singular value decomposition (SVD), thus obviating the need to repeatedly compute using a computational electromagnetic code and repeatedly solve a large method of moments matrix system at each point within the wide band of interest. The fast multipole method is used to obtain the solution vectors at these samples and speed up the matrix-vector product in the characteristic basis function method (CBFM). The resultant hybrid algorithm (FMM-CBFM) eliminates the need to generate and store the usual square impedance matrix and repeatedly use an iterative solver at each point and thus leads to a significant reduction in memory requirement and computational cost. Numerical examples are given to illustrate the accuracy and robustness of this method.

1 Introduction

2 The Fast Multipole Method

3 The Characteristic Basis Function Method

4 The Hybrid Method Combining the Fast Multipole Method and the Characteristic Basis Function Method

5 Discussions of the Parameters in the CBFM

6 Numerical Results

7 Conclusion

References

1. INTRODUCTION

The method of moments (MoM) has been widely used for the analysis of microstrip structures. However, the numerical solution of the MoM matrix equation requires $O(N^3)$ operations and $O(N^2)$ memory to store the matrix elements. The large operation count and memory requirement render the MoM solutions for large-scale problems prohibitively expensive. When an iterative solver is employed for solving the MoM matrix equation, the operation count is $O(N^2)$ per iteration because of the need to evaluate the matrix-vector multiplication. This operation count is too high for an efficient simulation.

To make the iterative method more efficient, it is necessary to speed up the matrix-vector multiplication. There are several techniques developed for this purpose, including the adaptive integral method (AIM) [1], the fast multipole method (FMM) [2,3], the impedance matrix localization (IML) [4], the conjugate-gradient fast Fourier transform method (CG-FFT) [5], and the precorrected-FFT method [6]. Recently, efforts have been made to extend these fast algorithms to microstrip problems. One such example is [7] where the FMM is adopted to analyze radiation from microstrip antennas with the aid of the discrete complex image method (DCIM) [8]. In this paper, the fast multipole algorithm is extended to solve scattering problems in microstrip environment. Though the FMM reduces memory requires and speeds up the matrix-vector multiplication, an iterative solver has to be adopted repeatedly at each point within the wide band of interest, and this, in turn, places an inordinately heavy burden on the CPU in terms of time, especially when the convergence rate of the iterative solver is very slow and the wideband response is very complicated in nature. Furthermore, it is very difficult to find a general iterative solver and preconditioner which is very efficient for all problems at an arbitrary frequency point.

One of the popular techniques for realizing a fast parameter sweep is the asymptotic waveform evaluation (AWE) technique [9]. This technique has been extended to the MoM solution of scattering from microstrip antennas so that the reduced order model is obtained to efficiently evaluate the frequency response over a broadband [10]. However, in the AWE algorithm, the LU factorization of the impedance matrix is necessary, and the derivative of the impedance matrix

with respect to the parameter must also be computed and stored, which make AWE only applicable to problems involving small matrix dimensions. However, for large finite arrays of microstrip antennas, the number of unknowns could run into over several thousands, the application of AWE to matrix equations resulting from the MoM has been rather limited. Furthermore, for microstrip structures, it is very difficult to compute the monostatic RCS using AWE because the high order derivative of the excitation vector with respect to the incident angle must be calculated. In addition, it is also difficult to combine AWE with AIM or FMM or other fast algorithms to obtain the wide responses. Another approach aimed at enhancing the computational efficiency in wide band is the adaptive sampling algorithm [11]. This method may need a lot of sample points when the response is very complex. Furthermore, it is very difficult to determine the accuracy of solutions in this method.

In this paper, we introduce a new fast and efficient hybrid algorithm combining the fast multipole method (FMM) and the characteristic basis function method (CBFM) [12] for analysis of scattering from microstrip antennas over a given wide band. In this method, the characteristic bases (CBs) are constructed firstly from the solution vectors at several samples using the singular value decomposition (SVD), and the current at any other sample points within the band is expressed as a linear combination of the CBs, which thus obviates the need to repeatedly solve a large method of moments matrix system at each sample point. Then, to make this algorithm applicable to large-scale structures, the FMM is used to obtain the solutions at several selected samples, and speed up the matrix-vector multiplication in the CBFM at the remaining points. Hence, the resultant hybrid algorithm (FMM-CBFM) eliminates the need to generate and store the usual square impedance matrix and calculate repeatedly with an iterative solver and thus leads to a significant reduction in memory requirement and computational cost. Furthermore, even if CBFM does not give the accuracy solution at some point within the band, the current at this point expressed as a linear combination of the CBs will be a more efficient initial guess which can help reduce the number of iterations over a typical choice of a zero initial guess. Several typical examples demonstrate the efficiency and accuracy of the proposed technique.

2. THE FAST MULTIPOLE METHOD

Consider a general microstrip structure residing on an infinite substrate having relative permittivity ϵ_r and thickness h . The microstrip is in the

x - y plane and excited by an applied field E^a . The induced current on the microstrip can be found by solving the well-known mixed potential integral equation (MPIE) [13]. First, the microstrip is divided into triangular elements and then the current is expanded using RWG basis functions [14]. Applying the Galerkin's method results in a matrix equation

$$ZI = V \quad (1)$$

in which the impedance matrix has the elements given by

$$Z_{ij} = j\omega \int_{T_i} \int_{T_j} \left[\vec{f}_i(\vec{r}) \cdot \overline{\overline{G}}_A(\vec{r}, \vec{r}') \cdot \vec{f}_j(\vec{r}') - \frac{1}{\omega^2} \nabla \cdot \vec{f}_i(\vec{r}) \nabla \cdot \vec{f}_j(\vec{r}') G_q(\vec{r}, \vec{r}') \right] dr' dr \quad (2)$$

where \vec{f}_i and \vec{f}_j represent the testing and basis function, respectively, T_i and T_j denote their supports, $\overline{\overline{G}}_A$ is the Green's function for vector potential, and G_q is the Green's function for scalar potential. In general, both $\overline{\overline{G}}_A$ and G_q can be expressed as an inverse Hankel transform of their spectral domain counterparts, which is commonly known as the Sommerfeld integral (SI). The analytical solution of the SI is generally not available, and the numerical integration is time consuming. This problem can be alleviated using DCIM [8], which yields closed-form expressions as

$$G(\vec{r}, \vec{r}') = \sum_{p=0}^{N_c} a_p \frac{e^{-jk r_p}}{4\pi r_p}, \quad r_p = |\vec{r} - (\vec{r}' + \hat{z} b_p)| \quad (3)$$

where a_p and b_p are the complex coefficients obtained from DCIM.

To use FMM, we first divide the entire structure into groups denoted by $G_m (m = 1, 2, \dots, M)$. Letting \vec{r}_i be the field point in a group centered at \vec{r}_m and \vec{r}_j be the source point in a group centered at $\vec{r}_{m'}$, we have

$$\begin{aligned} \vec{r}_{ij} &= \vec{r}_i - (\vec{r}_j + \hat{z} b_p) = (\vec{r}_i - \vec{r}_m) + (\vec{r}_m - \vec{r}_{m'}) + (\vec{r}_{m'} - \vec{r}_j) - \hat{z} b_p \\ &= \vec{r}_{im} + \vec{r}_{mm'} - \vec{r}_{jm'} - \hat{z} b_p \end{aligned} \quad (4)$$

Employing the addition theorem [2], we can rewrite the Green's function in (3) as

$$G(\vec{r}_i, \vec{r}_j) \approx \frac{k}{j16\pi^2} \oint \sum_{p=0}^{N_c} a_p e^{-j\vec{k} \cdot \hat{z} b_p} \times e^{-j\vec{k} \cdot (\vec{r}_{im} - \vec{r}_{jm'})} T(\hat{k} \cdot \hat{r}_{mm'}) d^2 \hat{k} \quad (5)$$

where

$$T(\hat{k} \cdot \hat{r}_{mm'}) = \sum_{l=0}^L (-j)^l (2l+1) h_l^{(2)}(\vec{k} \cdot \vec{r}_{mm'}) P_l(\hat{k} \cdot \hat{r}_{mm'}) \quad (6)$$

Substituting (5) into (2), we obtain

$$\begin{aligned} Z_{ij} = & \frac{\omega k}{16\pi^2} \left[\oint S_A(\hat{k}) U_{im}(\hat{k}) \cdot T(\hat{k}, \hat{r}_{mm'}) U_{jm'}^*(\hat{k}) d^2\hat{k} \right. \\ & \left. - \frac{1}{\omega^2} \oint S_q(\hat{k}) V_{im}(\hat{k}) \cdot T(\hat{k}, \hat{r}_{mm'}) V_{jm'}^*(\hat{k}) d^2\hat{k} \right] \quad (7) \end{aligned}$$

where

$$\begin{aligned} U_{im}(\hat{k}) &= \int_{T_i} e^{-j\vec{k} \cdot \vec{r}_{im}} \vec{f}_i(\vec{r}) d\vec{r}, \\ V_{im}(\hat{k}) &= \int_{T_i} e^{-j\vec{k} \cdot \vec{r}_{im}} \nabla \cdot \vec{f}_i(\vec{r}) d\vec{r} \quad \text{and} \quad S(\hat{k}) = \sum_{p=0}^{N_c} a_p e^{-j\vec{k} \cdot \vec{z}_{bp}} \end{aligned}$$

When an iterative method is used to solve (1), the matrix-vector multiplication can be performed in such a way that the contributions from nearby groups are calculated directly and the far interactions are calculated using (7).

In this algorithm, the image sources are grouped with the original source and hence the translation keeps unchanged for different images. Obviously, the algorithm requires little extra computation compared with that applied to free space problems. However, the method above is often affected by complex images' locations. To overcome this problem, a simple and efficient scheme presented in [15] can be used.

3. THE CHARACTERISTIC BASIS FUNCTION METHOD

To obtain the responses over a band of interest, we have to repeat the calculation at each discrete point. This will be very time consuming for the electromagnetic devices with complicated responses. To alleviate this problem, the characteristic basis function method [12] is proposed. To derive a parameter-independent characteristic basis set, we first compute the solution vectors by using the MoM at the starting (f_1) and ending (f_M) points. At the first level of the binary tree, an additional point is added at the center by averaging f_1 and f_M . Repeating the procedure to level m gives us $2^m + 1$ samples. Let $I^{(m)}$ be the current expansion coefficient vectors at level m . The set of vectors $\{I^{(m)}(f_i)\}$,

with $i = 1, \dots, 2^m + 1$ define a reduced-order subspace $\Xi^{(m)}$ of the original Hilbert space span

$$\Xi^{(m)} = \text{span}\{I^{(m)}(f_i)\} \quad (8)$$

If too few basis vectors are chosen, there would be an unacceptable loss of accuracy in the representation of $I(f)$. In order to define an orthonormal basis of $\Xi^{(m)}$, vectors $\{I^{(m)}(f_i)\}$ are arranged columnwise in a matrix A of size $N \times M$, where $M = 2^m + 1$. Next, the SVD of A is carried out as follows:

$$A = U \Sigma V^H \quad (9)$$

where U and V are unitary, and $\Sigma = \text{diag}(\sigma_1, \dots, \sigma_r)$, $r = \min(N, M)$ with $\sigma_1 \geq \sigma_2 \geq \dots \geq \sigma_r \geq 0$.

However, different from the circuit problems, the current coefficients for the scattering problems are very small because a plane wave with a unit magnitude is often used as the excitation. In fact, the elements of A are often on the order of $1.0\text{E-}3 \sim 1.0\text{E-}4$ and thus it is invalid to implement directly SVD of A . To overcome this problem, a simple and efficient method is introduced here that the elements of A can be largened by multiplying a large constant such as $1.0\text{E+}4$.

Then the current at any other point within the band of interest is approximated as a linear combination of the individual columns of U that form a characteristic basis specific to the geometry

$$I(f) = [U_1 \quad U_1 \quad \dots \quad U_M] \alpha^T \quad (10)$$

where U_1, U_1, \dots, U_M are the column vectors, and α is an complex expansion coefficient vector to be determined.

Equation (10) is substituted into (1), giving rise to a $M \times M$ linear system of algebraic equations after taking inner products with each of the characteristic basis

$$\begin{bmatrix} \langle U_1^H Z U_1 \rangle & \dots & \langle U_1^H Z U_p \rangle \\ \vdots & \vdots & \vdots \\ \langle U_p^H Z U_1 \rangle & \dots & \langle U_p^H Z U_p \rangle \end{bmatrix} \begin{bmatrix} \alpha_1 \\ \vdots \\ \alpha_M \end{bmatrix} = \begin{bmatrix} \langle U_1^H V \rangle \\ \vdots \\ \langle U_p^H V \rangle \end{bmatrix} \quad (11)$$

The above equation is solved for the α 's, which, when substituted in (10), gives the solution at the point of interest within the band from which the scattering responses can be easily evaluated.

4. THE HYBRID METHOD COMBINING THE FAST MULTIPOLE METHOD AND THE CHARACTERISTIC BASIS FUNCTION METHOD

Obviously, the CBFM above obviates the need to repeatedly solve a large method of moments matrix system at each point within the wide band of interest. In this method, the computationally intensive parts are comprised of (i) the computation of the solution vectors at samples, and (ii) the fill of the impedance matrix and the matrix-vector multiplications at other points. Hence it is still expensive for the direct analysis of electrically large problems. In addition, the impedance matrix must also be stored in this method. These make this algorithm only applicable to small or moderate structures.

On the other hand, though the FMM reduces memory requires and speeds up the matrix-vector multiplication, an iterative solver has to be adopted repeatedly at each point within the wide band of interest, and this, in turn, places an inordinately heavy burden on the CPU in terms of time, especially when the convergence rate of the iterative solver is very slow and the wideband response is very complicated in nature.

It is clear that if the CBFM is combined with the FMM, their advantages are both used. In this resultant hybrid algorithm, the FMM is used firstly to obtain the solution vectors at sample points and then speed up the matrix-vector product in CBFM at other points and an iterative solver with a preconditioner can be avoided. Furthermore, even if CBFM does not give the accuracy solution at some point within the band, the current at this point expressed as a linear combination of the CBs will be a more efficient initial guess which can help reduce the number of iterations over a typical choice of a zero initial guess. Hence, this hybrid algorithm (FMM-CBFM) eliminates the need to generate and store the usual square impedance matrix and calculate repeatedly at each discrete point using an iterative solver and thus leads to a significant reduction in memory requirement and computational cost.

5. DISCUSSIONS OF THE PARAMETERS IN THE CBFM

The singular vectors in U define a set of orthogonalized problem-matched basis functions of the reduced-order subspace. The dynamic range of the singular values ($\log(\sigma_1/\sigma_M)$) is a strong indicator of the span of the CBs, as has been demonstrated in [12]. However, it should be also noted that the large dynamic range of the singular values does not always mean that the solution is correct. We find

that the dynamic range of the singular values required to accurately simulate the structure is dependent on the scattering responses and the bandwidth. Hence, to determine more efficiently the accuracy of the solution, the residual ε of the matrix system (1) is evaluated using the solution obtained from (10). Here the residual ε is defined as follows:

$$\varepsilon = \frac{\|ZX - V\|_2}{\|V\|_2} \quad (12)$$

In this paper, our numerical experiments involving wide frequency scattering problems reveal that the residual will be so large at resonant frequency points that it is very difficult to determine the accuracy of the solution even if a lot of frequency samples are selected if they are not near these resonant frequency points. On the other hand, using only a few frequency samples, the characteristic basis function method can give the correct results at non-resonant frequency points. Based on the discussion above, we can start to estimate the solution at other frequencies by using the CBs constructed by several samples. If the residual in (12) is not met at some frequency point, we can include it in the CBs by carrying out the SVD on this new set. The process is gone on until all the solutions are obtained with the small residuals. In this method, by placing new samples at the larger value of the residual, this residual is minimized with respect to frequency. In fact, these new samples often lie near the resonance frequency points. Hence this algorithm automatically selects and minimizes the number of sample points. Furthermore, the adaptive algorithm does not require any a priori knowledge.

Our numerical experiments reveal when $(\log(\sigma_1/\sigma_M))$ reaches to 2, the basis vectors have sufficient span at non-resonant frequency points. Hence this condition is chosen in this paper. However, numerical experiments in [12] involving the circuit problems revealed that this number should be at least 3 to ensure that the basis vectors have sufficient span. It is clear that for the scattering problems, constraint can be relaxed. If this condition is not met, we move to the next level of the binary tree by adding additional frequency samples, which, in turn, expands the dynamic range. Of course, we also think that sample points are enough if the solution obtained from (10) gives small residual at a new sample point. This often takes place when the monostatic RCS from microstrip structures is considered or the band of interest is very narrow.

On the other hand, in the conventional iterative solvers, e.g., the CG scheme, ε is chosen to be on the order of 0.5%–1% to obtain an accurate solution vector. One of the reasons for imposing such a stringent condition is to prevent the CG scheme from getting trapped

in local minima. However, our studies indicate that this constraint can be relaxed to 15%–20% in the present approach because the solution is tightly controlled by the CBs constructed from the solutions at other points — and this represents an important advantage. Of course, if the solution constructed from the CBs is not sufficiently accurate, we proceed to compute it using FMM, and then include it in the CBs by carrying out the SVD on this new set. Here, the current at this point expressed as a linear combination of the CBs is a more efficient initial guess which can help reduce the number of iterations over a typical choice of a zero initial guess.

It should also be noted that if the band of interested is too much wide, more basis vectors must be chosen to ensure the accuracy in the representation of the solutions at non-sample points. Because the CPU time is proportional to the number of CBFs in the CBFM, it is desirable to keep the number of sample points as small as possible. To alleviate this problem, the entire band can be divided into several sub-bands so that only a few CBs are needed in each sub-band and then the computing efficiency is enhanced furthermore.

6. NUMERICAL RESULTS

To illustrate the validity and accuracy of the method described above, we present several typical numerical examples. All of the computations are performed on a PC equipped with 512 MB of RAM and a 2.4-GHz processor. As a first example, we consider the scattering from a circle patch microstrip antenna with the radius of 7.1 mm. The substrate parameters are $h = 0.7874$ mm and $\varepsilon_r = 2.2$. The patch is illuminated by an θ -polarized incident plane wave traveling along the direction of $\theta^i = 63^\circ$ and $\varphi^i = 0^\circ$.

A modeling of this structure requires 492 unknowns, and it remains unchanged over the frequency range of interest, which is from 6 to 18 GHz in steps of 100 MHz. Because this structure is too small and thus the method of moments is adopted to obtain the solutions at sample points instead of the fast multipole method. We begin by computing the current on the structure at 6 and 18 GHz directly by solving (1). In the first level, an additional frequency point at 12 GHz is added and its solution is constructed from the CBs derived from 6 and 18 GHz. The residual is found to be unacceptable and, hence, the MoM matrix system is solved directly. We then go to the second level by adding two more frequency points at 9 and 15 GHz, respectively. At 9 GHz, the residual also turns out to be high, and we then compute the solution directly. Now the dynamic range increases to 2.0954, as shown in Fig. 1, and we thus stop sampling. At this stage, we solve (1) directly

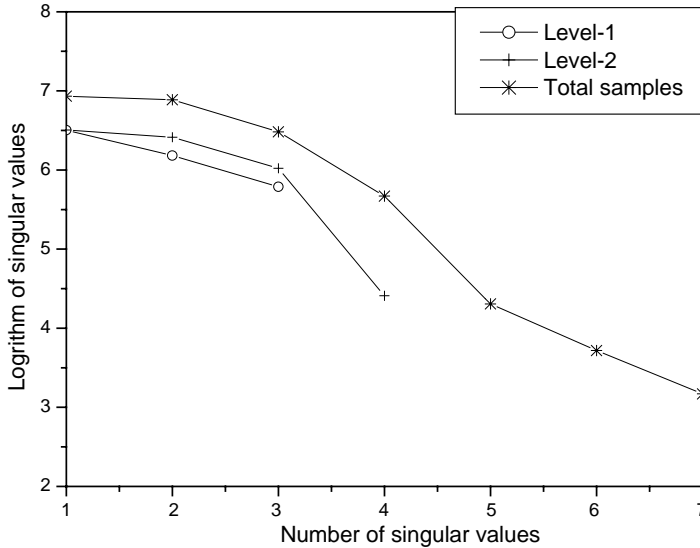


Figure 1. Distribution of singular values at various levels for the circle patch.

at four frequency points, and construct four CBs. The distribution of singular values at each of the levels is presented in Fig. 1, and it can be seen that the dynamic range ($\log(\sigma_1/\sigma_M)$) increases with adding more frequency points. The ratio is just 0.71487 at level 1, while it increases to 3.7629 finally.

Next, the solution is constructed at other frequencies by using the four CBs without directly solving (1). The residual is evaluated over the entire band, and presented in Fig. 2. This figure shows that the residual is within 20% over the entire frequency band except at 7.7, 12.6 and 13.5 GHz. Hence at these three frequency points, the solution vectors are also computed directly and included in the CBs by carrying out the SVD on this new set. In contrast, the iterative solvers such as the CG method use a residual criterion of 1% to terminate the iterations. In fact, in the present algorithm, this condition can be relaxed to 20% without loss of accuracy. This is demonstrated by computing the scattering responses from the circle patch, and the results obtained are presented in Fig. 3, and are seen to be indistinguishable from those of direct calculation and the results in [16] over the entire frequency band of interest.

The CPU time for the direct solution of (1) at each frequency point is 0.44s, and the time taken to evaluate the response at 121 frequency

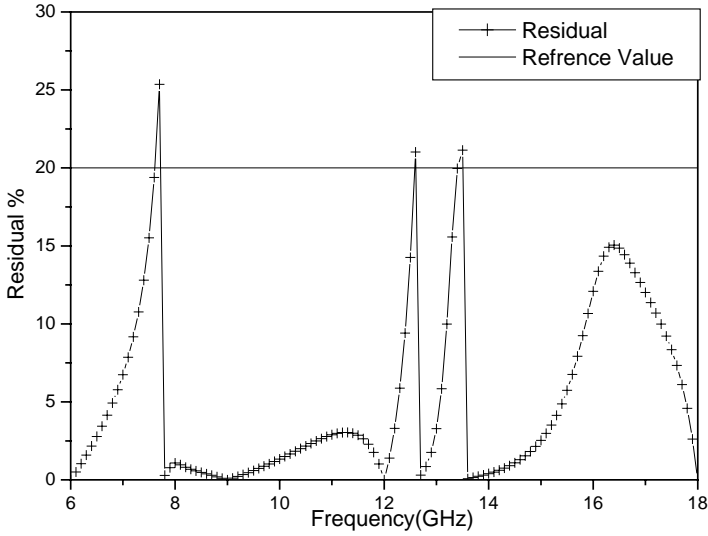


Figure 2. Percentage residual of the MoM system versus frequency for the circle patch.

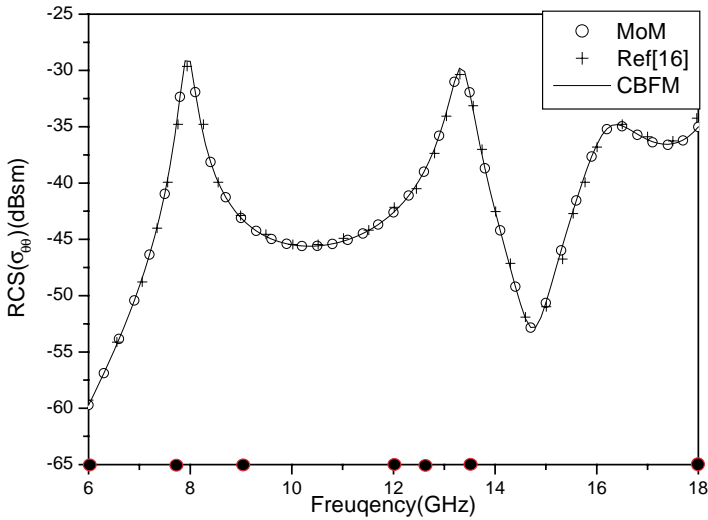


Figure 3. RCS versus frequency for the circle patch using CBFM and MoM.

points is 53.24 s. The present approach involves computing the solution directly at seven frequency samples, and the solution at any desired frequency f in the range $6.0 < f < 7.7$ GHz is constructed from the four CBs, and in the range $7.7 < f < 9.0$ GHz is constructed from the five CBs and so on. The CBFM takes just 0.0 s, 0.05 s, 0.05 s and 0.06 s at each frequency sample point if four, five, six and seven CBs are used respectively. The total time for computing the response over the entire frequency band is 8.96 s, which makes the present approach more than 5.9 times faster than the direct computation.

Then we consider the plane wave scattering from two finite arrays of microstrip patch antennas. The element of the arrays is a rectangular patch with 36.6 mm width and 26.6 mm length. The distance between two adjacent elements in both the x and y directions is 55.517 mm. The geometry can be obtained from [17]. The substrate parameters are $h = 1.58$ mm and $\epsilon_r = 2.17$. In the FMM, the group size d is $0.25\lambda_0$ with λ_0 being the wavelength in free space. The number of modes L is chosen to be $k_0d + 3\ln(\pi + k_0d)$. The patch is illuminated by an θ -polarized incident plane wave traveling along the direction of $\theta^i = 0^\circ$ and $\varphi^i = 45^\circ$. The 3×3 and 7×7 arrays are considered and they have 1737 and 9457 unknowns respectively and are analyzed from 2 to 4 GHz in steps of 50 MHz leading to a total of 41 frequency points. Similarly, three samples are selected using the adaptive algorithm above, and the dynamic range increases to 2.20749 and 2.21428 respectively, for the 3×3 and 7×7 arrays, as shown in Fig. 4. The residual of (12) is found to be less than 20% from 2 to 4 GHz except at 2.75 GHz (see Fig. 5). Hence the FMM is employed to compute the current at this point, and then include it in the CBs. The currents at the remaining 37 frequency points are constructed by using the CBs, and then the scattering responses are computed. The RCS as a function of frequency is presented in Fig. 6, by using the present approach, along with the MoM solution and the results in [17]. An excellent agreement is showed over the entire frequency band.

It should be noted that in the FMM, to speed up the convergence rate of iterative solvers such as the generalized minimal residual (GMRES), the incomplete LU (ILU) preconditioner with a dual dropping strategy is used [18]. In the ILUT preconditioner, the dual dropping strategy is implemented using the two parameters τ and p , where τ is the threshold drop tolerance and p is the fill-in parameter. Here we select $\tau = 0.01$ and $p = 0$. The iterative numbers are 3, 5, 12, 12 and 3, 5, 9, 14 with a zero initial guess for the 3×3 and 7×7 arrays at four sample frequencies, respectively. In fact, we can use the current expressed as a linear combination of the CBs as an initial guess after the second sample points. Then the iterative numbers are 3, 5, 8, 10 and 3,

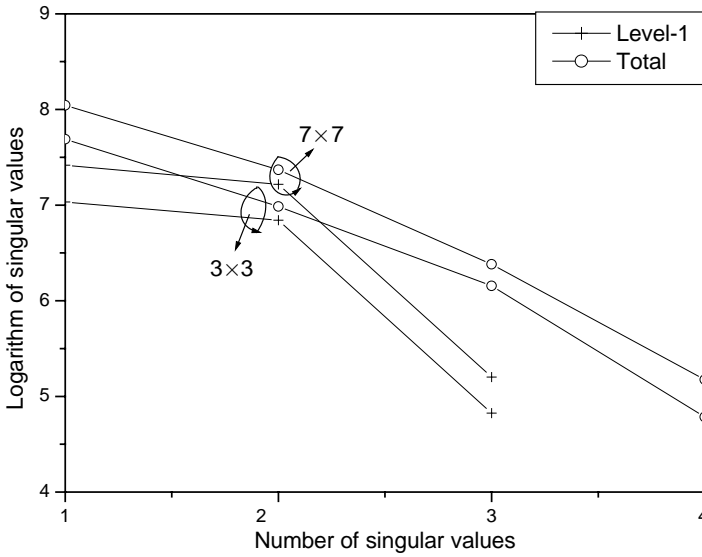


Figure 4. Distribution of singular values at various levels for the 3×3 and 7×7 arrays.

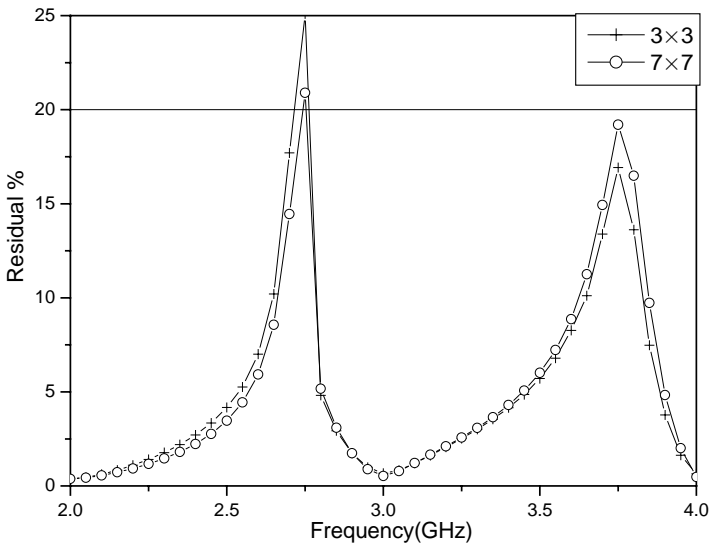


Figure 5. Percentage residual of the MoM system versus frequency for the 3×3 and 7×7 arrays.

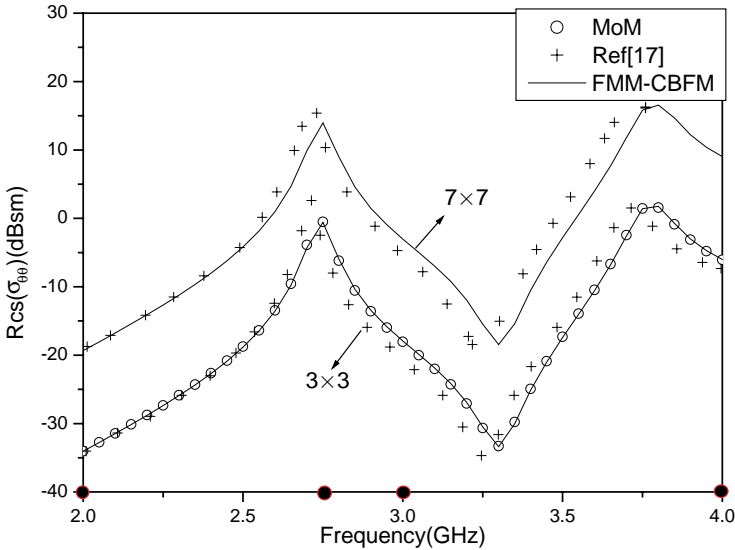


Figure 6. RCS versus frequency for the 3×3 and 7×7 arrays using FMM-CBFM and MoM.

5, 6, 12 for them respectively. Hence this initial guess is more efficient than a zero initial guess. On the other hand, in the FMM-CBFM, the main operation involves just M matrix-vector products and the iterative process and preconditioning can be avoided and thus enhance the compute efficiency. To illuminate this, the iterative numbers over the entire frequency band are plotted in Fig. 7. In these two examples, the maximum number of iterations to allow is 500. Hence it is very clear that the convergence is not achieved at three frequencies. However, the iterative process can be avoided in our method and only several CBs are used to construct the solutions at these three frequencies and thus the computing time can be saved. In fact, the present approach takes just 0.55 s and 0.76 s for the 3×3 array and 15.66 s and 17.68 s for the 7×7 array when three CBs and four CBs are used respectively. At the same time, it should be noted that the convergence can be achieved by choosing a smaller value of τ and a larger value of p in the ILUT implementation at these three frequencies. However, this means more time and memory must be spent on preconditioning.

The monostatic RCS ($\sigma_{\theta\theta}$) as functions of θ for these two arrays at 3.7 GHz is also considered. The distribution of singular values finally is presented in Fig. 8 and Fig. 9 at $\phi = 0^\circ$ and $\phi = 90^\circ$, respectively, and it can be easily seen that the dynamic range is very small. However,

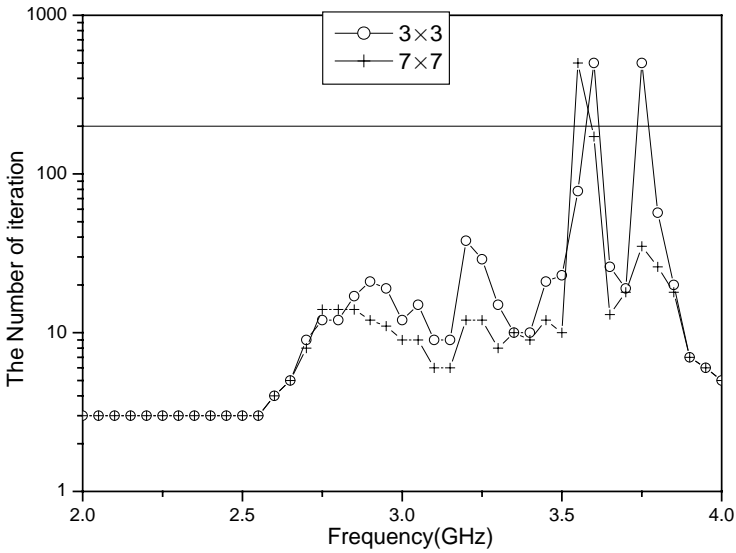


Figure 7. The iterative number versus frequency for the 3×3 and 7×7 arrays

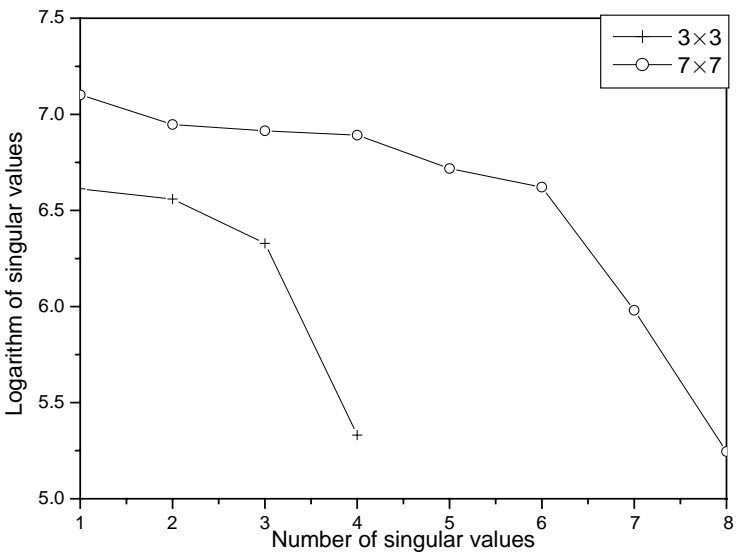


Figure 8. Distribution of singular values at various levels at $\phi = 0^\circ$.

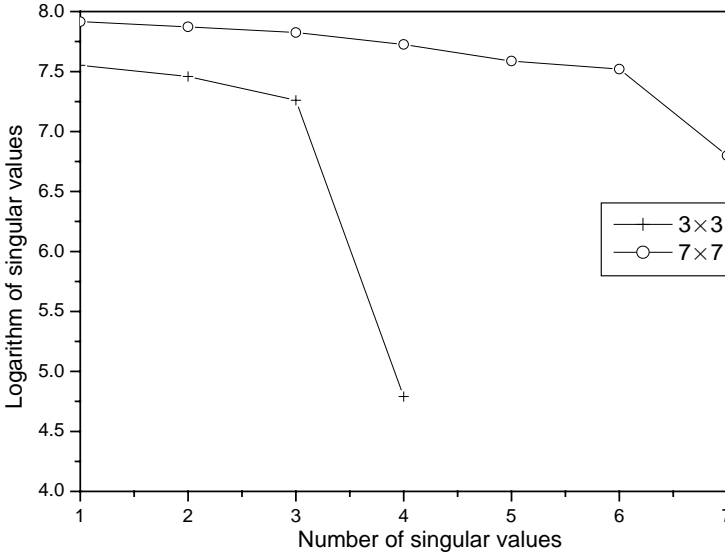


Figure 9. Distribution of singular values at various levels at $\phi = 90^\circ$.

the solution obtained from (10) gives small residual ($< 20\%$) at 5th and 8th sample point for the 3×3 and 7×7 arrays, respectively. Hence, we think that these sample points are also enough to ensure that the basis vectors have sufficient span. The residual ε is evaluated over the entire band, and presented in Fig. 10 and Fig. 11. At $\phi = 0^\circ$ and $\theta = 3^\circ$, the residual exceeds 20% for the 7×7 array and thus the current is solved using FMM at this point, and then include it in the CBs by carrying out the SVD on this new set. The solutions are shown in Fig. 12 and Fig. 13, respectively. Since 3.7 GHz corresponds to the (0,1) cavity mode resonance, the broadside response is greatest at $\phi = 90^\circ$ and least at $\phi = 0^\circ$. The results obtained by King and Bow [17] and Ling and Jin [19] are also given in the figures for comparison. It is observed that our results agree very well with those given in [17] and [19]. The iterative numbers and the CPU time at the last sample point are tabulated in Table 1 using the initial guess from CBFM and compared to a zero initial guess. We can see clearly the efficiency of the initial guess from CBFM again. The CPU time for FMM solution of (1) is also given in this table for comparison with our method in which four CBs are used and take just 0.93 s for the 3×3 array and seven CBs or eight CBs are used and take just 28.61 s or 32.90 s for the 7×7 array. Hence this hybrid algorithm is very efficient.

On the other hand, the monostatic RCS ($\sigma_{\theta\theta}$) as functions of θ will

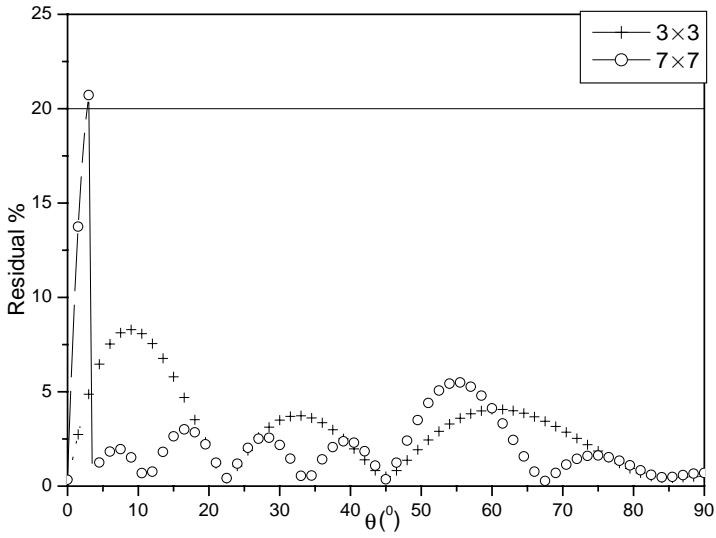


Figure 10. Percentage residual of the MoM system versus frequency at $\phi = 0^\circ$.

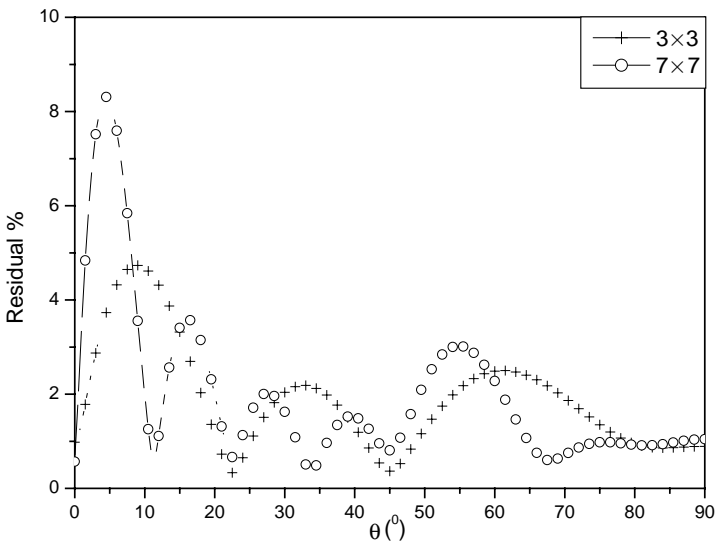


Figure 11. Percentage residual of the MoM system versus frequency at $\phi = 90^\circ$.

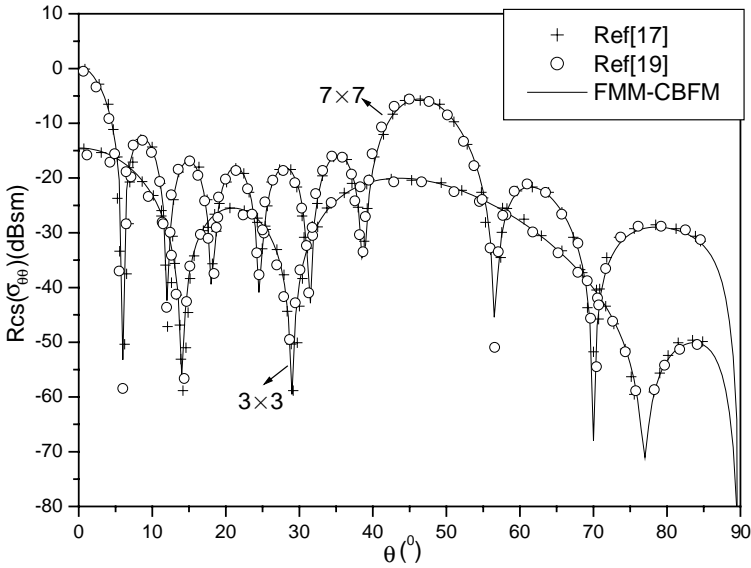


Figure 12. RCS versus θ for various size arrays at $\phi = 0^\circ$.

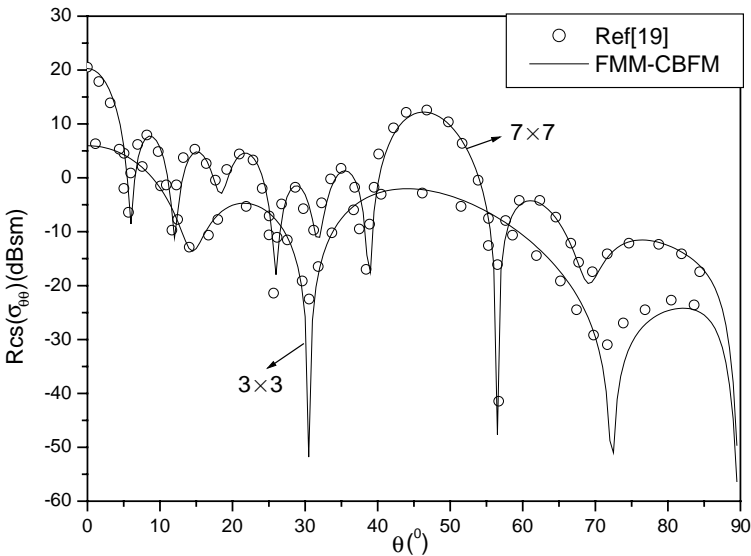


Figure 13. RCS versus θ for various size arrays at $\phi = 90^\circ$.

Table 1. Comparison of the number of iteration and CPU Time (s) for FMM-CBFM and FMM

Examples	The 3×3 array		The 7×7 array	
	$\phi = 0^\circ$	$\phi = 90^\circ$	$\phi = 0^\circ$	$\phi = 90^\circ$
The number of iteration with a zero initial guess	17	28	14	18
The time of solving of (1)	5.19	8.29	80.75	95.73
The number of iteration with a initial guess from CBFM	15	12	9	18
The time of solving of (1)	4.67	4.07	59.71	95.73

get more complex with increasing the size of the array and thus more CBs must be chosen to ensure that these basis vectors have sufficient span which will lead to the degraded efficiency of CBFM. To alleviate this problem, the entire band can be divided into several sub-bands so that only a few CBs are needed in each sub-band and the computing efficiency is enhanced furthermore.

7. CONCLUSION

An efficient hybrid algorithm combining the fast multipole method (FMM) and the characteristic basis function method for fast computation of the response of large-scale microstrip structures over a wide band has been presented. The approach has involved expanding the current at any point within the band as a linear combination of the CBs that are constructed from the SVD of the solutions obtained at a few other sampling points. The fast multipole method is used to obtain the solution vectors at these samples and speed up the matrix-vector product in the characteristic basis function method (CBFM). The resultant hybrid algorithm (FMM-CBFM) eliminates the need to generate and store the usual square impedance matrix and repeatedly use an iterative solver at each point and thus leads to a significant reduction in memory requirement and computational cost. Representative numerical results are presented and illustrate the accuracy and computational efficiency of the proposed technique.

REFERENCES

1. Bleszynski, E., M. Bleszynski, and T. Jaroszewicz, "AIM: adaptive integral method for solving large-scale electromagnetic scattering and radiation problems," *Radio Sci.*, Vol. 31, 1225–1251, Sept./Oct. 1996.
2. Coifman, R., V. Rokhlin, and S. Wandzura, "The fast multipole method for the wave equation: A pedestrian prescription," *IEEE Antennas Propagat. Mag.*, Vol. 35, No. 3, 7–12, June 1993.
3. Song, J. M., C. C. Lu, and W. C. Chew, "Multilevel fast multipole algorithm for electromagnetic scattering by large complex objects," *IEEE Trans. Antennas Propagat.*, Vol. 45, No. 10, 1488–1493, Oct. 1997.
4. Canning, F. X., "The impedance matrix localization (IML) method for moment-method calculations," *IEEE Antennas Propagat. Mag.*, Vol. 32, 18–30, Oct. 1990.
5. Sarkar, T. K., E. Arvas, and S. M. Rao, "Application of FFT and the conjugate gradient method for the solution of electromagnetic radiation from electrically large and small conducting bodies," *IEEE Trans. Antennas Propagat.*, Vol. 34, No. 5, 635–640, May 1986.
6. Phillips, J. R. and J. K. White, "A precorrected-FFT method for electrostatic analysis of complicated 3-D structures," *IEEE Trans. Computer-Aided Design of Integrated Circuits and Systems*, Vol. 16, No. 10, 1059–1072, Oct. 1997.
7. Ling, F., J. Song, and J.-M. Jin, "Multilevel fast multipole algorithm for analysis of large-scale microstrip structures," *IEEE Microwave Guided Wave Lett.*, Vol. 9, No. 12, 508–510, Dec. 1999.
8. Chow, Y. L., J. J. Yang, D. G. Fang, and G. E. Howard, "A closed-form spatial Green's function for the thick microstrip substrate," *IEEE Trans. Microwave Theory Tech.*, Vol. 39, No. 3, 588–592, Mar. 1991.
9. Pillage, L. T., et al., "Asymptotic waveform evaluation for timing analysis," *IEEE Trans. Comput.-Aided Des. integrated Circuits and Syst.*, Vol. 9 No. 4, 352–366, April 1990.
10. Wan, J. X. and C. H. Liang, "Rapid solutions of scattering from microstrip antennas using well-conditioned asymptotic waveform evaluation," Accepted by *Journal of Electromagnetic Waves and Applications*, 2004.
11. Lehmensiek, R. and P. Meyer, "An efficient adaptive frequency sampling algorithm for model-based parameter estimation as applied to aggressive space mapping," *Microwave Opt. Technol.*

- Lett.*, Vol. 24, No. 1, 71–78, Jan. 2000.
12. Prakash, V. V. S., J. Yeo, and R. Mittra, “An adaptive algorithm for fast frequency response computation of planar microwave structures,” *IEEE Trans. Microwave Theory Tech.*, Vol. 52, No. 3, 920–926, Mar. 2004.
 13. Mosig, J. R., “Arbitrarily shaped microstrip structures and their analysis with a mixed potential integral equation,” *IEEE Trans. Microwave Theory Tech.*, Vol. 36, No. 2, 314–323, Feb. 1988.
 14. Rao, S. M., D. R. Wilton, and A. W. Glisson, “Electromagnetic scattering by surfaces of arbitrary shape,” *IEEE Trans. Antennas and Propagat.*, Vol. 30, No. 3, 409–418, 1982.
 15. Wan, J. X., T. M. Xiang, and C. H. Liang, “Fast multipole algorithm for analysis of large-scale microstrip antennas arrays,” accepted by *Journal of Electromagnetic Waves and Applications*, 2004.
 16. Wang, C. F., F. Ling, and J. M. Jin, “A fast full-wave analysis of scattering and radiation from large finite arrays of microstrip antennas,” *IEEE Trans. Antennas Propagat.*, Vol. 46, No. 10, 1467–1474, Oct. 1998.
 17. King, A. S. and W. J. Bow, “Scattering from a finite array of microstrip patches,” *IEEE Trans. Antennas Propagat.*, Vol. 40, No. 7, 770–774, July 1992.
 18. Saad, Y., “ILUT: a dual threshold incomplete LU factorization,” *Numer. Linear Algebra Appl.*, Vol. 1, 387–402, 1994.
 19. Ling, F. and J. M. Jin, “Scattering and radiation analysis of microstrip antennas using discrete complex image method and reciprocity theorem,” *Microwave Opt. Technol. Lett.*, Vol. 16, No. 4, 212–216, Nov. 1997.

Wan Jixiang was born in Henan, China, on May 25, 1978. He received the B.S. and M.S. degrees in electrical engineering from XiDian University, Xi’an, China, in 2000 and 2003, respectively. And he currently is pursuing Ph.D. degree at XiDian University. His research interests include numerical methods for electromagnetic, microstrip antennas, and microwave and millimeter-wave integrated circuits.

Liang Changhong was born in Shanghai, China, on December 9, 1943. He graduated in 1965 from the former Xidian University, Xi’an, China, and continued his graduate studies until 1967. From 1980 to 1982, he worked at Syracuse University Syracuse, New York, USA as a visiting scholar. He has been a professor and Ph.D. student advisor of

Xidian University since 1986. He was awarded the titles “National Middle-Aged and Young Expert with Distinguished Contribution”, “National Excellent Teacher”, and “One of the 100 National Prominent Professors”, etc. Prof. Liang has wide research interests, which include computational microwave and computational electromagnetics, microwave network theory, microwave measurement method and data processing, lossy variational electromagnetics, electromagnetic inverse scattering, electromagnetic compatibility. Prof. Liang is a Fellow of CIE and a Senior Member of IEEE.

Lei Juan was born in Shanxi, China, 1979. She received the B.S. and M.S. degrees in electrical engineering from XiDian University, Xi’an, China, in 2000 and 2003, respectively. Since 2003, she has worked at the National Key Laboratory of Antennas and Microwave Technology at XiDian University. And her research interests include the analysis and design of phased arrays, waveguide slot antennas, microstrip antennas, and microwave integrated circuit analysis.